University of South Bohemia in České Budějovice

Faculty of Science

Mathematical modelling of the population dynamics of hemiparasitic plants

Bachelor thesis

Mgr. Petra Světlíková

Supervisor: doc. Ing. Luděk Berec, Dr.

České Budějovice 2014

Světlíková, P., 2014: Mathematical modelling of the populaton dynamics of hemiparasitic plants. Bc. Thesis, in English. – 32 p., Faculty of Science, University of South Bohemia, České Budějovice, Czech Republic.

Annotation

The hemiparasite-host interaction is rather complex, acting as parasitism belowground and as competition for light aboveground. Studies modelling this interaction are rare. The most recent model of the hemiparasite-host interaction was developed from the well-known Rosenzweig-MacArthur predator-prey model by Fibich et al. (2010). Here, I modified the light availability function of the model into a more general form and examined the hemiparasite-host coexistence along a productivity gradient of the environment. The behaviour of presented and analyzed model was shown to depend particularly on parameter g_∞ scaling light availability for hemiparasites at high host biomasses. While it suggested the host-hemiparasite coexistence only at intermediate productivities under low g_∞, species could coexist even at high productivities under higher g_∞.

Prohlášení

Prohlašuji, že svoji bakalářskou práci jsem vypracovala samostatně pouze s použitím pramenů a literatury uvedených v seznamu citované literatury.

Prohlašuji, že v souladu s § 47b zákona č. 111/1998 Sb. v platném znění souhlasím se zveřejněním své bakalářské práce, a to v nezkrácené podobě elektronickou cestou ve veřejně přístupné části databáze STAG provozované Jihočeskou univerzitou v Českých Budějovicích na jejích internetových stránkách, a to se zachováním mého autorského práva k odevzdanému textu této kvalifikační práce. Souhlasím dále s tím, aby toutéž elektronickou cestou byly v souladu s uvedeným ustanovením zákona č. 111/1998 Sb. zveřejněny posudky školitele a oponentů práce i záznam o průběhu a výsledku obhajoby kvalifikační práce. Rovněž souhlasím s porovnáním textu mé kvalifikační práce s databází kvalifikačních prací Theses.cz provozovanou Národním registrem vysokoškolských kvalifikačních prací a systémem na odhalování plagiátů.

České Budějovice, December 9, 2014

.....

Petra Světlíková

Acknowledgements

I would like to thank to my supervisor, Luděk Berec, for his help and valuable advice during the work on this thesis. I am also grateful to Šuspa and Pavel Fibich for giving me advice when I needed it.

Contents

1 Introduction

1.1 *Parasitic plants*

Parasitism is an extraordinary life strategy, where one species, the parasite, exploits another species, the host. Parasites usually refer to animal species as helminths or nematodes or to tiny organisms as bacteria or viruses. However, parasitic species can be also found in plant kingdom. More than 4000 of flowering plants are parasitic, acquiring some (hemiparasites) or all (holoparasites) resources from other plant species (Heide-Jørgensen, 2013). The vast majority of plant parasites are hemiparasites, green plants which obtain a significant portion of their resources heterotrophically (Heide-Jørgensen, 2013). Water, diluted mineral nutrients, and heterotrophic carbon are among essential resources that hemiparasites acquire from their host species through specialized organs (Press, 1989; Irving and Cameron, 2009; Těšitel et al., 2010). These organs called haustoria are attached to host stems by stem-hemiparasites, and to host roots by root-hemiparasites.

Root-hemiparasites are recognized as an important functional group of hemiparasites, affecting key ecosystem processes such as nutrient cycling (Press, 1998; Quested et al., 2005; Bardgett et al., 2006; Demey et al., 2014), competition among resident plants (Gibson and Watkinson, 1991; Pywell et al., 2004), and ecosystem biodiversity and productivity (Davies et al., 1997; Joshi et al., 2000; Ameloot et al., 2005; Mudrák and Lepš, 2010). Several genera of root-hemiparasites from the Orobanchaceae family commonly occur throughout Europe in natural and seminatural habitats. Although they are generalists, exploiting many co-occurring host species at the same time, some host species can be preferred and some avoided (Cameron et al., 2006; Rümer et al., 2007; Thorogood and Hiscock, 2010). Hemiparasites can even parasitise on other hemiparasites (Prati et al., 1997). In order to survive, hemiparasites have to find host plants and attach to them as soon as possible after their germination (Press and Phoenix, 2005). However, many hemiparasites can survive an initial seedling stage without any host plant (Press, 1989; Press and Phoenix, 2005).

1.2 *Mathematical models*

A mathematical model is a simplified and purposeful mathematical representation of a real system that we are interested in. The real system described in such a way, e.g. by means of differential equations, can be subsequently examined and thus better understood. Mathematical models are very useful tools in many scientific disciplines. In biology, they are used mostly for the following purposes. They help to explain system functioning, examine interactions and relationships between system components, find patterns that are not apparent from the data, predict system behaviour under specific conditions, test hypotheses that cannot be tested experimentally, verify existing theories, and establish new ones. If the biological system is modelled by means of differential equations, the solution of which can be found either analytically or by adequate numerical methods, that solution then determines system behaviour over time.

1.3 *Modelling of the hemiparasite-host interaction*

The hemiparasite-host interaction is rather complex, functioning mainly as resource parasitism belowground and as competition for light aboveground (Fibich et al., 2010). Both the hemiparasite and host species are able to uptake resources from soil, but this source is utilized almost exclusively by the host. The hemiparasite acquires most of its resources by exploiting the host (Cameron and Seel, 2007; Westwood, 2013). Since hemiparasites are generally weak competitors (Atsatt and Strong, 1970; De Hullu, 1984), the aboveground interaction tends to be asymmetric. According to Smith (2000), deficits in parasite competitive abilities may be overcome by resource parasitism.

The hemiparasite-host interaction is shaped by abiotic factors, e.g. productivity of the environment (Cameron et al., 2005). It is well known that the aboveground competition becomes more important when nutrient availability is increased (Grime, 1979; Keddy et al., 1997; Wilson and Tilman, 1991). Taking into account poor competitive abilities of hemiparasites, it is not surprising that hemiparasites preferably occur in low-productivity habitats. In high-productivity environments, strong shading by the host species cannot be further compensated by resource parasitism (Yeo, 1964; Van Hulst et al., 1987; Fürst, 1931).

There are only a few studies modelling the hemiparasite-host relationship. A simple model of resource-based competition was proposed by Smith (2000). That model considered only the

belowground interaction and a single resource limiting the plant populations. It also assumed that the hemiparasite could complete its life cycle without any host, become more abundant with increasing productivity, and outcompete the host. Cameron et al. (2009) suggested a spatial model examining the interaction between a parasite and two host plant types (forbs and grasses) under two nutrient levels. They parameterized the model with the data from a pairwise interaction experiment where the hemiparasite was grown with three different grass and forb species. The model exhibited highly unstable dynamics under the high nutrient level, but stable dynamics under the low nutrient level. The most recent model of the hemiparasite-host interaction was developed by Fibich et al. (2010). It involved both above- and belowground interactions and removed the assumptions made by Smith (2000) which were not consistent with field observations. The model behaviour was examined on a productivity gradient corresponding to the host carrying capacity. The model showed that both plant types can coexist only at intermediate productivities, otherwise only the host species survives. At very low productivities, there are not enough hosts to sustain the hemiparasitic species. At the other extreme, hemiparasites are shaded by hosts and thus excluded from highly productive sites. Fibich et al. (2010) emphasized that the addition of light competition component to the model was a key step in order to explain field observations. Important role of light competition in the hemiparasite-host relationship was previously suggested also by Matthies (1995).

Here, I generalize the light availability function for the hemiparasite used by Fibich et al. (2010) and examine the hemiparasite-host coexistence along the productivity gradient. This generalization enables the hemiparasite to assure some light also at high host densities and the hemiparasite response to changing host density may vary from gradual to abrupt. The resulting model is mathematically analysed applying the isoclines analysis, the analysis of equilibrium points and the bifurcation analysis.

The thesis is divided into several sections. Relevant mathematical concepts and theorems, and the original and modified models of the hemiparasite-host interaction are presented in Sections 2 and 3, respectively. The generalized model is mathematically analysed in Section 4. The model results are discussed and compared with similar models in Section 5, where the model limitations are also specified and possible improvements of the model are suggested. In Section 6, I summarize the main results of the thesis.

2 Relevant mathematical concepts and theorems

I start with definitions of the nonlinear systems of autonomous ordinary differential equations and a solution of these systems, followed by theorems and definitions regarding the existence and stability of the solutions of these differential equations, equilibrium points, and bifurcations.

Definition 1. (Nonlinear systems of autonomous ordinary differential equations, Perko (2001), p. 65) Let E be an open subset of R^n and $f : E \to R^n$. Then systems of autonomous ordinary differential equations of the first order and resolved with respect to the derivative are systems of equations of the form

$$\dot{x} = f(x). \tag{1}$$

From here on, I will speak of the systems (1) simply as of differential equations.

Definition 2. (Solution of differential equation, Perko (2001), p. 71) Suppose that $f \in C(E)$ where E is an open subset of R^n. Then $x(t)$ is a solution of the differential equation

$$\dot{x} = f(x) \tag{2}$$

on an interval I if $x(t)$ is differentiable on I and if for all $t \in I$, $x(t) \in E$ and

$$x'(t) = f(x(t)).$$

And given $x_0 \in E$, $x(t)$ is a solution of the initial value problem

$$\begin{aligned} \dot{x} &= f(x) \\ x(0) &= x_0 \end{aligned}$$

on an interval I if $0 \in I$, $x(0) = x_0$ and $x(t)$ is a solution of the differential equation (2) on the interval I.

Theorem 2. (The fundamental existence-uniqueness theorem, Perko (2001), p. 74) Let E be an open subset of R^n containing x_0 and assume that $f \in C^1(E)$. Then there exists an $a > 0$ such that the initial value problem

$$\begin{aligned} \dot{x} &= f(x) \\ x(0) &= x_0 \end{aligned} \tag{3}$$

has a unique solution $x(t)$ on the interval $[-a, a]$.

Theorem 3. (Perko (2001), p. 89) Let E be an open subset of R^n and assume that $f \in C^1(E)$. Then for each point $x_0 \in E$, there is a maximal interval J on which the initial value problem (3) has a unique solution, $x(t)$; i.e., if the initial value problem has a solution $y(t)$ on the interval I then $I \subset J$ and $y(t) = x(t)$ for all $t \in I$. Furthermore, the maximal interval J is open; i.e., $J = (\alpha, \beta)$.

Definition 3. (Perko (2001), p. 90) The interval (α, β) in Theorem 3 is called the maximal interval of existence of the solution $x(t)$ of the initial value problem (3) or simply the maximal interval of existence of the initial value problem (3).

A standard way to start analyzing a nonlinear system of differential equations $\dot{x} = f(x)$ is to determine its equilibrium points and describe its behaviour near these equilibrium points.

Definition 4. (Perko (2001), p. 102) A point $x_0 \in R^n$ is called an equilibrium point of (1) if $f(x_0) = 0$. An equilibrium point x_0 is called a hyperbolic equilibrium of (1) if none of the eigenvalues of the matrix $Df(x_0)$ have zero real part.

Here the matrix $Df(x_0)$ is the Jacobian matrix defined as

$$Df(x_0) = J(x_0) = \begin{pmatrix} \frac{\partial f_1}{\partial x_1} & \cdots & \frac{\partial f_1}{\partial x_n} \\ \vdots & \ddots & \vdots \\ \frac{\partial f_n}{\partial x_1} & \cdots & \frac{\partial f_n}{\partial x_n} \end{pmatrix}$$

where $f = (f_1, \ldots, f_n)$ and f_i for $i = 1, ..., n$ are functions of $x = (x_1, ..., x_n)$.

Definition 5. (Perko (2001), p. 102) An equilibrium point x_0 of (1) is called a sink if all of the eigenvalues of the matrix $Df(x_0)$ have negative real part; it is called a source if all of the eigenvalues of $Df(x_0)$ have positive real part; and it is called a saddle if it is a hyperbolic equilibrium point and $Df(x_0)$ has at least one eigenvalue with a positive real part and at least one eigenvalue with a negative real part. The linear system $\dot{x} = Ax$ with the matrix $A = Df(x_0)$ is called the linearization of (1) at x_0.

Theorem 4. (The Hartman-Grobman theorem, Mathematical analysis IV, Lecture notes) Assume a nonlinear system of differential equations in the form

$$\dot{x} = Ax + g(x)$$

where $g(0) = 0$ and g is a continuous function for which

$$\lim_{\|x\| \to 0} \frac{\|g(x)\|}{\|x\|} \to 0.$$

Then the zero solution of (1) is locally asymptotically stable if all of the eigenvalues of the matrix A have negative real part, and unstable if at least one eigenvalue has a positive real part.

Combining Definition 4, Definition 5 and Theorem 4, the following theorem shows that near a hyperbolic equilibrium point x_0, the nonlinear system $\dot{x} = f(x)$ has the same qualitative structure as its linearization $\dot{x} = Ax$ with $A = Df(x_0)$.

Theorem 5. (Perko (2001), p. 129) Let x_0 be a hyperbolic equilibrium point and $Re(\lambda_j)$ denote the real part of the eigenvalue λ_j of the matrix $Df(x_0)$, $j = 1, ..., n$. Then the hyperbolic equilibrium point x_0 is asymptotically stable if $Re(\lambda_j) < 0$ for all $j = 1, ..., n$, thus if x_0 is a sink. And the hyperbolic equilibrium point x_0 is unstable if $Re(\lambda_j) > 0$ for at least one $j \in 1, ..., n$, thus if x_0 is a source or a saddle.

To assess the stability of equilibrium points, we need not calculate exact eigenvalues of the corresponding Jacobian matrix. The knowledge of their signs suffices. The Routh-Hurwitz criterion gives necessary and sufficient conditions for local asymptotic stability of an equilibrium, i.e. for real parts of all of the eigenvalues of the corresponding Jacobian matrix to be negative. For two-dimensional systems of differential equations, this criterion is as follows:

$$det(Df(x_0)) > 0 \text{ and } trace(Df(x_0)) < 0 \tag{4}$$

In the analysis of our generalized hemiparasite-host population model, we will commonly encounter two types of bifurcations, a fold (or saddle-node) bifurcation and a supercritical Hopf bifurcation. To help understand the fold (saddle-node) bifurcation, consider an autonomous system of ordinary differential equations (Kuznetsov, 2010)

$$\dot{x} = f(x, \alpha), x \in R^1, \alpha \in R^1 \tag{5}$$

with a smooth function f, which has at $\alpha = 0$ the equilibrium $x = 0$ with $\lambda = f_x(0, 0) = 0$. Let for $\alpha < 0$ the system have two equilibria (one stable and one unstable). Also, while α crosses zero from negative to positive values, let the two equilibria collide and disappear, forming at $\alpha = 0$ an equilibrium with $\lambda = 0$ (Fig. 1). This behaviour of the system (5) is called a fold or saddle-node bifurcation (Kuznetsov, 2010). The point at which $\alpha = 0$ and simple equilibrium $\lambda = 0$ exists is commonly referred to as a limit point.

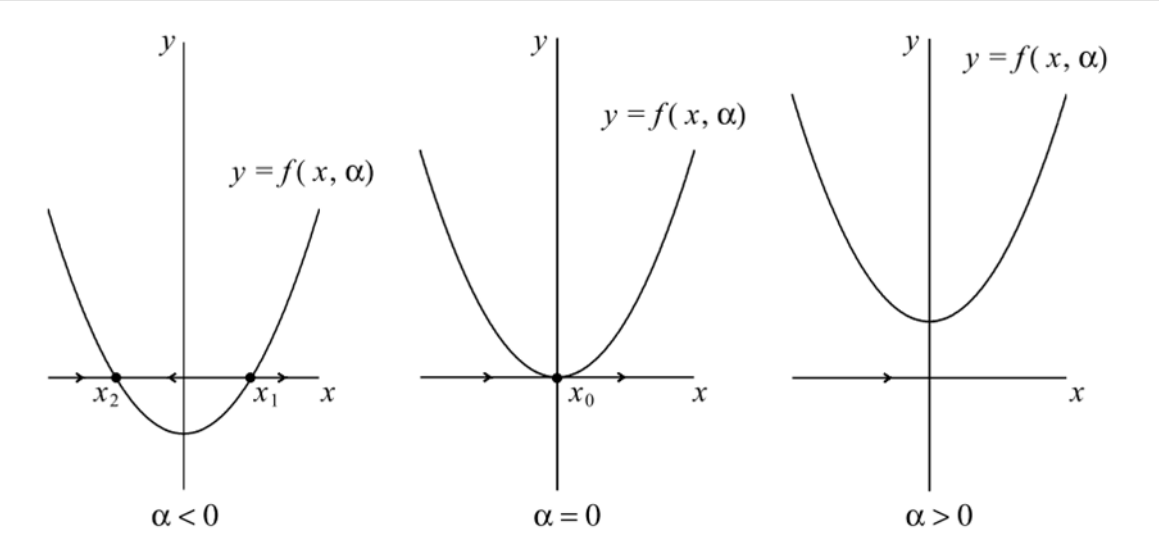

Figure 1: Fold (saddle-node) bifurcation). Reprinted from Kuznetsov (2010).

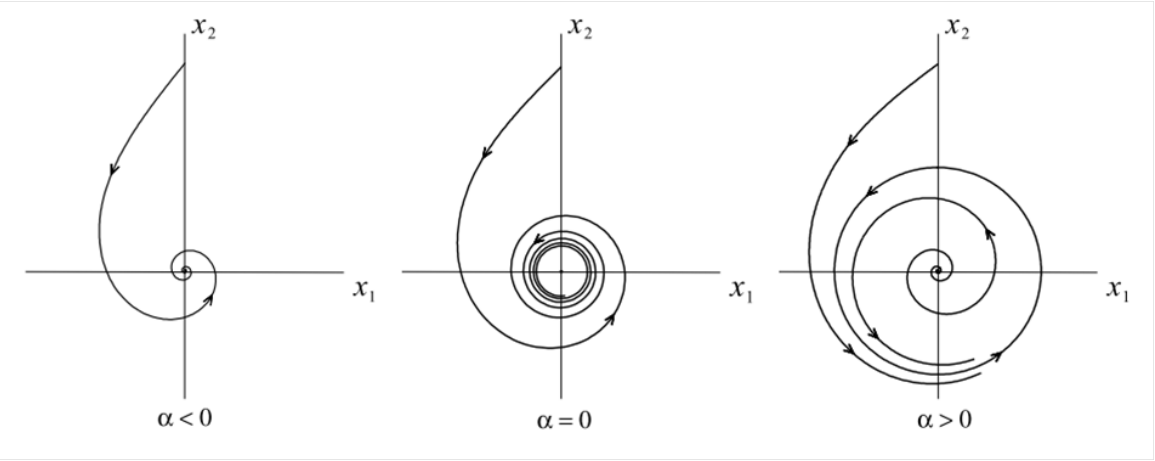

Figure 2: Supercritical Hopf bifurcation. Reprinted from Kuznetsov (2010).

To help understand the supercritical Hopf bifurcation, consider an autonomous system of or-

dinary differential equations (Kuznetsov, 2010)

$$\dot{x} = f(x, \alpha), x = (x_1, x_2)^T \in R^2, \alpha \in R^1 \tag{6}$$

with a smooth function f, which has at $\alpha = 0$ the equilibrium $x = 0$ with eigenvalues $\lambda_{1,2} = \pm i\omega_0$, $\omega_0 > 0$. Let this equilibrium be linearly stable if $\alpha < 0$ and unstable for $\alpha > 0$, surrounded by a stable limit cycle (Fig. 2). This behaviour of the system (6) is called a supercritical Hopf bifurcation (Kuznetsov, 2010). The point at which $\alpha = 0$ and $\lambda_{1,2} = \pm i\omega_0$, $\omega_0 > 0$ is referred to as a Hopf point.

3 Methods

A mathematical model describing the hemiparasite-host interaction was developed by Fibich et al. (2010) from the Rosenzweig-MacArthur predator-prey model. The Rosenzweig-MacArthur predator-prey model consists of the logistic growth of prey and the type II functional and numerical responses of predators (Rosenzweig and MacArthur, 1963; Kot, 2001):

$$\begin{aligned} \frac{dx}{dt} &= rx\left(1-\frac{x}{K}\right) - f(x)y \\ \frac{dy}{dt} &= -my + ef(x)y \end{aligned} \tag{7}$$

In this original model, x and y represent prey and predator densities, respectively, r is the intristic prey growth rate in the absence of predation, K is the carrying capacity of prey in the absence of predation, m is the per capita mortality rate of predators in the absence of prey, and e is the efficiency of converting consumed prey into new predators. Finally, $f(x)$ is the type II functional response:

$$f(x) = \frac{ax}{x+b}$$

where a denotes the maximum per capita predation rate and b the host density necessary to achieve one-half of this maximum rate.

The model by Fibich et al. (2010) considers host plants as prey and hemiparasitic plants as predators. The predator mortality rate m is defined as a decrease of hemiparasite biomass. The host biomass is proportional to the amount of host resources (water and nutrients), which can be taken up by the hemiparasite. The host biomass decreases when these resources are acquired by the hemiparasite. The efficiency of the hemiparasite to uptake resources and convert them into its own biomass is denoted as e.

Fibich et al. (2010) included competition for light and parasitism among hemiparasites into the original predator-prey model as follows:

$$\begin{aligned} \frac{dx}{dt} &= rx\left(1-\frac{x+cy}{K}\right) - f(x)y \\ \frac{dy}{dt} &= -(m+m_1 y)y + ef(x)yg(x) \end{aligned} \tag{8}$$

Here c expresses the competitive ability of hemiparasites for light relative to their hosts, m_1 refers to negative interactions among hemiparasites comprising intra-specific parasitism and competition for light, and $g(x)$ refers to a function scaling light availability and accounting for competitive ability of hosts for light relative to their hemiparasites (light is less available for hemiparasites with increased host biomass). They assumed the following sigmoidally decreasing form of $g(x)$ ranging from 1 to 0:

$$g(x) = 1 - \frac{x^2}{x^2 + d^2} = \frac{d^2}{x^2 + d^2} \tag{9}$$

where d refers to the host biomass necessary to achieve $g(x) = 1/2$. Hence, hemiparasites cannot survive in highly dense vegetation where their light availability declines to zero.

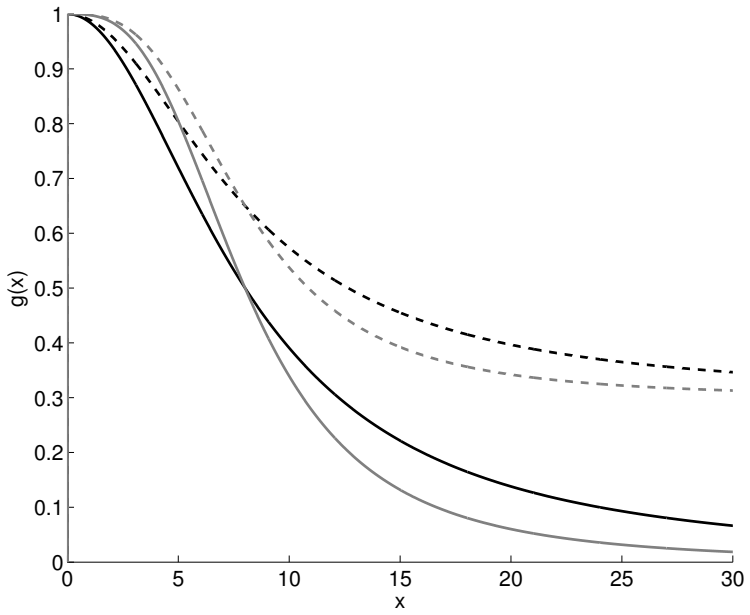

Figure 3: Light availability function $g(x)$ describing the decreasing light availability to hemiparasites with increasing host biomass x. Solid and dashed lines indicate the function where $g_\infty = 0$ and $g_\infty = 0.3$, respectively. Black colour corresponds to $z = 2$, while grey colour corresponds to $z = 3$.

Here, I assume a more general form of the light availability function $g(x)$:

$$g(x) = 1 - (1 - g_\infty)\frac{x^z}{x^z + d^z} = \frac{g_\infty x^z + d^z}{x^z + d^z} \tag{10}$$

For this function, $g(x)$ decreases to g_∞ in the limit $x \to \infty$, which may be $0 \leq g_\infty \leq 1$. Since $g'(d) = -(1 - g_\infty)\frac{z}{4d}$, the parameter z scales the rate at which the function $g(x)$ "falls" from

1 to g_∞. Note that the original function (9) is a special form of the new one (10) when we set $g_\infty = 0$ and $z = 2$. Several forms of the light availability function (10) are plotted in Fig. 3.

In general, the model (8) decribes the whole hemiparasite-host interaction using light as the aboveground limiting resource and water and nutrients as the belowground limiting resources. Without hemiparasites, host plants will grow logistically till they reach the carrying capacity of the environment K, which is determined by both groups of limiting resources. The carrying capacity of the host thus depends on the productivity of the environment.

The model (8) can be simplified by the transformation of some parameters and an appropriate scaling of time:

$$\bar{t} = rt; \overline{m} = m/r; \overline{m_1} = m_1/r; \overline{a} = a/r$$

Bars dropped, the final system has the following form:

$$\begin{aligned} \frac{dx}{dt} &= x\left(1 - \frac{x + cy}{K}\right) - \frac{ax}{x+b}\, y \\ \frac{dy}{dt} &= -(m + m_1 y)y + e\,\frac{ax}{x+b}\, y\,\frac{g_\infty x^z + d^z}{x^z + d^z} \end{aligned} \tag{11}$$

I analyze the model (11) in the next chapter.

4 Results

In this section, I analyze the model (11) and primarily focus on the effect of the host carrying capacity K. Some results are calculated numerically using Matlab (The MathWorks, Inc.) with Matcont package for bifurcation analysis (Dhooge et al., 2003) and Pplane package for visualization of isoclines and system dynamics (Polking and Arnold, 1999). I begin with the calculation of equilibrium points. Equilibrium points are located at the intersection of the host and hemiparasite isoclines.

4.1 *Isocline analysis*

The zero-growth isoclines are obtained by setting the right-hand sides of equations (11) to zero. There are two isoclines both for the host and the hemiparasite. One isocline for each species is trivial: $x = 0$ (the hemiparasite axis) and $y = 0$ (the host axis). The other, non-trivial isoclines are

$$y = \frac{(x+b)(K-x)}{xc+bc+aK} =: h(x,K) \tag{12}$$

for the host, and

$$y = \frac{1}{m_1}\left(\frac{(g_\infty x^z + d^z)eax}{(x+b)(x^z+d^z)} - m\right) =: p(x) \tag{13}$$

for the hemiparasite. I keep the parameter K as an argument of function $h(x,K)$ to emphasize that I will explore the model primarily with respect to it. Figures 4 and 5 show several specific forms of these isoclines.

The non-trivial host isocline (12) intersects the x (host) axis at $x = K$ and $x = -b$ and the y (hemiparasite) axis at

$$y = \frac{bK}{bc+aK} =: h(0,K) > 0$$

The first derivative of the non-trivial host isocline (12) is

$$h'(x,K) = \frac{-cx^2 - 2xbc - 2xaK - cb^2 - baK + aK^2}{(xc+bc+aK)^2} \tag{14}$$

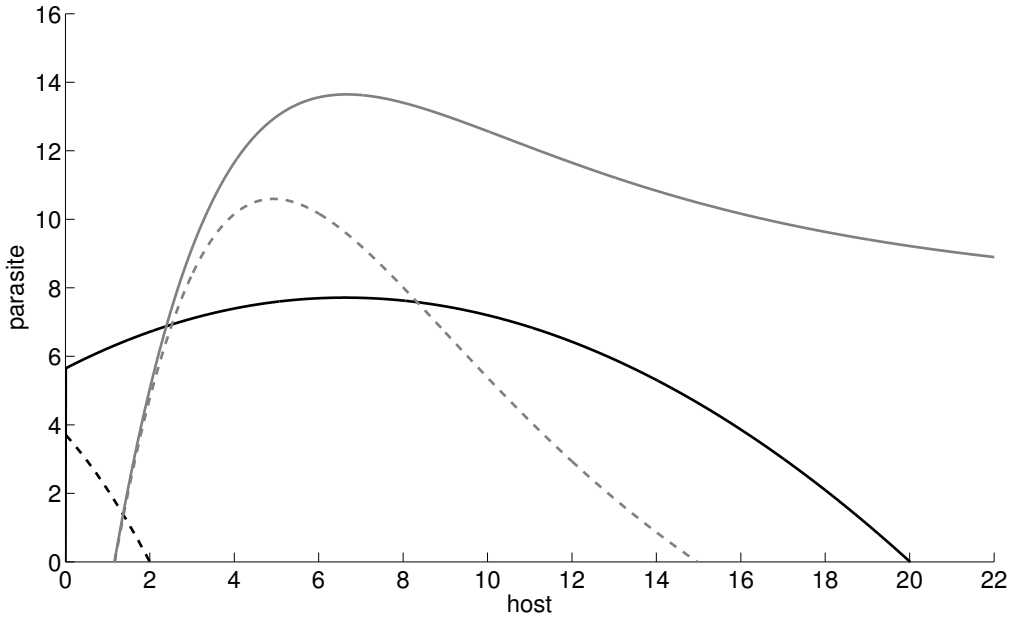

Figure 4: The host non-trivial isoclines (black) displayed for two different values of the host carrying capacity K ($K = 20$ and 2, solid and dashed, respectively) and the hemiparasite non-trivial isoclines (grey) displayed for two different values of parameter g_∞ ($g_\infty = 0.3$ and 0, solid and dashed, respectively). The rest of parameters was set as follows: $e = 1$, $a = 0.63$, $b = 6$, $d = 8$, $m = 0.1$, $m_1 = 0.01$, $c = 0.1$ and $z = 2$.

By putting $x = 0$, I analyze the behavior of the host isocline in its intersection with the y (hemiparasite) axis:

$$h'(0, K) = \frac{-cb^2 - baK + aK^2}{(xc + bc + aK)^2}$$

The host isocline intersects the y axis as an increasing function when its first derivative is positive, i.e. when

$$K \in \left(-\infty, \frac{b}{2}\left(1 - \sqrt{1 + \frac{4c}{a}}\right)\right) \cup \left(\frac{b}{2}\left(1 + \sqrt{1 + \frac{4c}{a}}\right), \infty\right) \tag{15}$$

On the contrary, the host isocline intersects the y axis as a decreasing function when its first derivative is negative, i.e. when

$$K \in \left(\frac{b}{2}\left(1 - \sqrt{1 + \frac{4c}{a}}\right), \frac{b}{2}\left(1 + \sqrt{1 + \frac{4c}{a}}\right)\right) \tag{16}$$

Notice that the left range in (15) and the lower bound of (16) are negative, which is biologically irrelevant. Therefore, the ranges at which the first derivative $h'(0, K)$ is either positive or

negative can be respectively simplified to

$$K \in \left(\frac{b}{2} \left(1 + \sqrt{1 + \frac{4c}{a}} \right), \infty \right)$$

and

$$K \in \left(0, \frac{b}{2} \left(1 + \sqrt{1 + \frac{4c}{a}} \right) \right)$$

By putting the first derivative (14) to zero, extremes can be found:

$$h'(x, K) = 0 \Leftrightarrow -cx^2 - 2xbc - 2xaK - cb^2 - baK + aK^2 = 0$$

which solves to

$$x_{1,2} = -b - \frac{aK}{c} \pm \frac{2}{c}\sqrt{aK(bc + aK + cK)}$$

To determine the types of these extremes, the second derivative has to be calculated:

$$h''(x, K) = -2\,\frac{abcK + aK^2 + acK^2}{(xc + bc + aK)^3}$$

From here

$$h''(x_1, K) < 0$$

$$h''(x_2, K) > 0$$

Thus, the non-trivial host isocline reaches its maximum in x_1 and the minimum in x_2. However, note that $x_2 < 0$; since $h(0, K) > 0$ we have $h(x, K) > 0$ for $x \in [0, K)$ and $h(x, K) < 0$ for $x > K$. In addition, $h''(x, K) < 0$ for $x \geq 0$. Hence, altogether, the host isocline (12) starts at $h(0, K) > 0$, is concave in $[0, \infty)$, intersects the x (host) axis at $x = K$, and becomes negative for $x > K$.

Intersection of the non-trivial hemiparasite isocline (13) with the x (host) axis cannot be determined analytically. According to the numerical calculations, there is at least one intersection point, which will be further denoted as point A. If the non-trivial hemiparasite isocline intersects the x axis twice, the second (larger) point will be denoted as B ($A < B$). The non-trivial hemiparasite isocline (13) intersects the y (hemiparasite) axis at

$$y \;=\; -\frac{m}{m_1} < 0$$

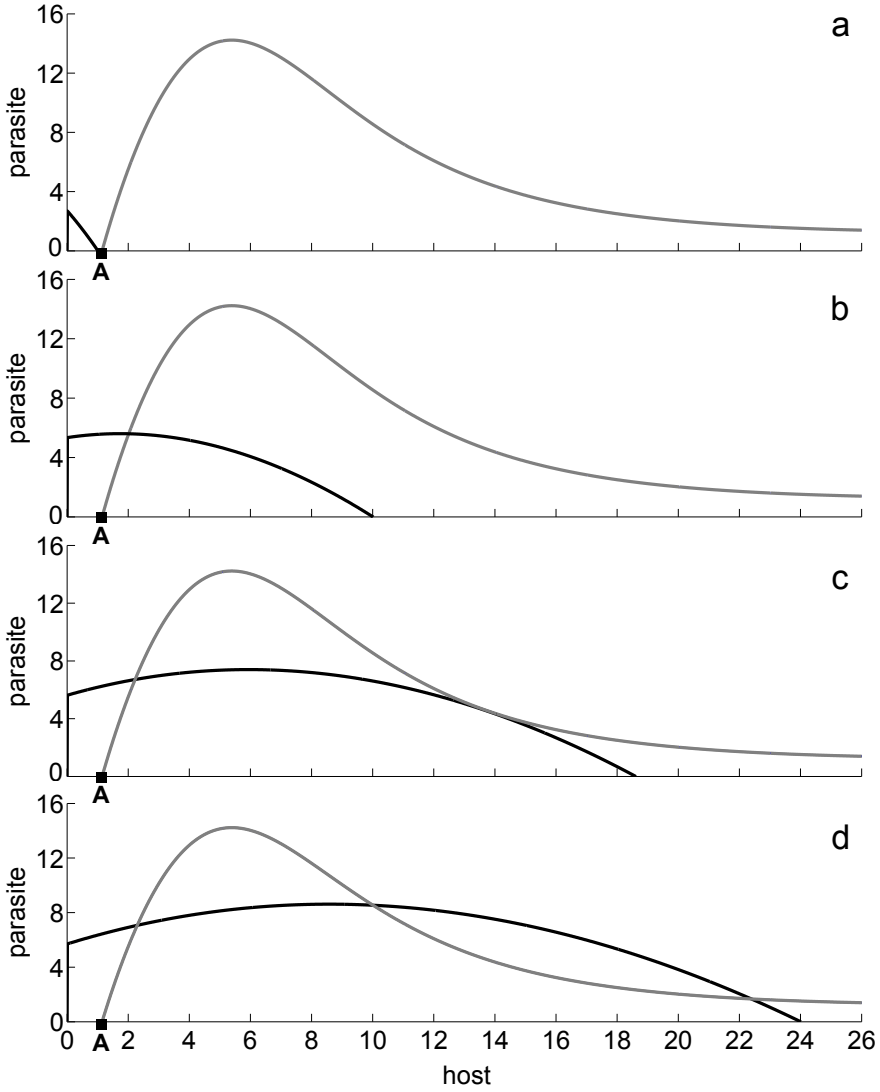

Figure 5: The host (black) and hemiparasite (grey) isoclines along an increasing productivity gradient and their intersections corresponding to the coexistence equilibria. The productivity gradient is implied by parameter K, the host carrying capacity. Parameters were set as follows: $e = 1$, $a = 0.63$, $b = 6$, $d = 8$, $m = 0.1$, $m_1 = 0.01$, $c = 0.1$, $z = 3$, $g_\infty = 0.2$, and $K = 1$ (a), $K = 10$ (b), $K = 20$ (c) and $K = 24$ (d).

The first derivative of the non-trivial hemiparasite isocline (13) is

$$p'(x) = \frac{ea[(g_\infty x^z + d^z + x^z z g_\infty)(x+b)(x^z+d^z) - x(x^z g_\infty + d^z)(x^z + d^z + (x+b)zx^{z-1})]}{m_1(x+b)^2(x^z+d^z)^2}$$

By putting $x = 0$, I analyze the behavior of the hemiparasite isocline at its intersection with the y (hemiparasite) axis:

$$p'(0) = \frac{ea}{m_1 b} \tag{17}$$

Taking into account that all model parameters are positive, the right-hand side of the equation (17) is always positive and the hemiparasite isocline always intersects the y axis as an increasing function.

Unfortunately, the extremes of (13) cannot be found analytically. According to the numerical calculations, the hemiparasite isocline has only one extreme, a maximum. In addition,

$$\lim_{x\to\infty} p(x) = \frac{eag_\infty - m}{m_1} =: p_\infty$$

It is obvious that p_∞ increases with increasing g_∞, and

$$p_\infty > 0 \Leftrightarrow g_\infty > \frac{m}{ea} \tag{18}$$

$$p_\infty < 0 \Leftrightarrow g_\infty < \frac{m}{ea} \tag{19}$$

4.2 *Trivial system equilibria*

Trivial system equilibria are the equilibria where one or both species become extinct. The model (11) has two trivial equilibria, $[0,0]$ and $[K,0]$, which always exist. The stability properties of the trivial equilibria are derived from the Jacobian matrix of the model (11):

$$J[x,y] = \begin{pmatrix} a_{11} & a_{12} \\ a_{21} & a_{22} \end{pmatrix}$$

where

$$\begin{aligned}
a_{11} &= 1 - \frac{x+cy}{K} + x\left(\frac{ay}{(x+b)^2} - \frac{1}{K}\right) - \frac{ay}{x+b} \\
a_{12} &= -x\left(\frac{c}{K} + \frac{a}{x+b}\right) \\
a_{21} &= -eayx^z \frac{g_\infty z + g_\infty + 2z + 1}{(x+b)(x^z+d^z)} \\
a_{22} &= -2ym_1 + eax\frac{g_\infty x^z + d^z}{(x+b)(x^z+d^z)} - m
\end{aligned}$$

The determinant of the Jacobian matrix evaluated at the extinction equilibrium $[0,0]$,

$$det\,(J[0,0]) = -m$$

is always negative. Therefore, the equilibrium $[0, 0]$ is unstable (saddle point) according to the Routh-Hurwitz criterion (4).

The determinant and trace of the Jacobian matrix evaluated at the trivial equilibrium $[K, 0]$ when the hemiparasite is missing is

$$\begin{aligned} det\,(J[K,0]) &= m - eaK\frac{g_\infty K^z + d^z}{(K+b)(K^z+d^z)} \\ trace\,(J[K,0]) &= -1 - m + eaK\frac{g_\infty K^z + d^z}{(K+b)(K^z+d^z)} \end{aligned}$$

which, using the hemiparasite isocline, can be expressed as

$$det\,(J[K,0]) = -p(K)m_1 \tag{20}$$

$$trace\,(J[K,0]) = p(K)m_1 - 1 \tag{21}$$

This implies that if $p(K) < 0$, $det\,(J[K,0]) > 0$ and $trace\,(J[K,0]) < 0$ and the equilibrium $[K, 0]$ is locally asymptotically stable. On the contrary, if $p(K) > 0$, $[K, 0]$ is unstable.

If $p_\infty < 0$ and the carrying capacity K is between A and B, the points for which $p(A) = p(B) = 0$, $p(x)$ is positive for any $x \in (A, B)$. Hence, the determinant of the Jacobian matrix (20) is negative and $[K, 0]$ is an unstable equilibrium for $K \in (A, B)$. However, if $p_\infty < 0$ and K lies outside the range (A, B), $p(x)$ is negative, the determinant of the Jacobian matrix (20) is positive and the trace (21) is negative. This indicates that $[K, 0]$ is a stable equilibrium for K outsite the range (A, B).

If $p_\infty > 0$ and $K > A$, $p(x)$ is positive for any $x > A$. Thus, the determinant of the Jacobian matrix (20) is negative and $[K, 0]$ is an unstable equilibrium for any $K > A$. Otherwise, if $p_\infty > 0$ and $K < A$, $p(x)$ is negative and $[K, 0]$ is a stable equilibrium for any $K < A$.

4.3 *Non-trivial system equilibria*

Non-trivial system equilibria are the equilibria at which both species coexist. These equilibria were determined using numerical methods, because the model (11) is too complex to do it

analytically. The model (11) was examined under similar parameter values as the original, simpler model of Fibich et al. (2010) (8) to enable their comparison. The parameters were set as follows: $e = 1$, $a = 0.63$, $b = 5$ or 6, $d = 8$, $m = 0.1$, $m_1 = 0.01$, and $c = 0.1$. The parameters g_∞ and z of the light availability function $g(x)$ and the host carrying capacity K were varied.

If $K < A$, there are no non-trivial equilibria, but only the unstable trivial equilibrium $[0, 0]$ and the stable trivial equilibrium $[K, 0]$. Therefore, only the host plant survives under low values of K and the host biomass grows to K. The host carrying capacity is too low to keep the hemiparasite alive.

The second intersection of the hemiparasite isocline (13) with the x axis, the point B exists only under low values of g_∞ (when $g_\infty < \frac{m}{ea} \approx 0.15$ for the adopted parameter values, 19). If K lies inside the range (A, B), the host-only equilibrium $[K, 0]$ is unstable and there is either one or three coexistence equilibria depending on the host carrying capacity K and the coefficient z. If there is only one coexistence equilibrium, it is stable or unstable. If there are three coexistence equilibria, the first one (corresponding to the lowest host biomass) can be stable or unstable, the second one with the intermediate host biomass is always unstable (saddle point), and the third one (corresponding to the highest host biomass) is always stable. If K lies outside the range (A, B), the host-only equilibrium $[K, 0]$ is stable and there can be two coexistence equilibria (Fig. 6). The first equilibrium $E1$ can be stable or unstable with a stable limit cycle around it and the second equilibrium $E2$ is always unstable (saddle point) (Fig. 6). No coexistence equilibrium exists for low values of g_∞ under high enough environmental productivity K.

If the point B does not exist (for $g_\infty > \frac{m}{ea}$, 18), the host-only equilibrium $[K, 0]$ is unstable and the host isocline intersects the hemiparasite isocline at one or three equilibrium points (Fig. 7). If they intersect only once, the coexistence equilibrium is stable or unstable under low K, but it is always stable under high K. If the isoclines intersect three times, the stability of equilibria is similar to the situation with three coexistence equilibria in the case of $K \in (A, B)$: the first one (corresponding to the lowest host biomass) can be stable or unstable, the second one with the intermediate host biomass is always unstable (saddle point), and the third one (corresponding to the highest host biomass) is always stable (Fig. 7).

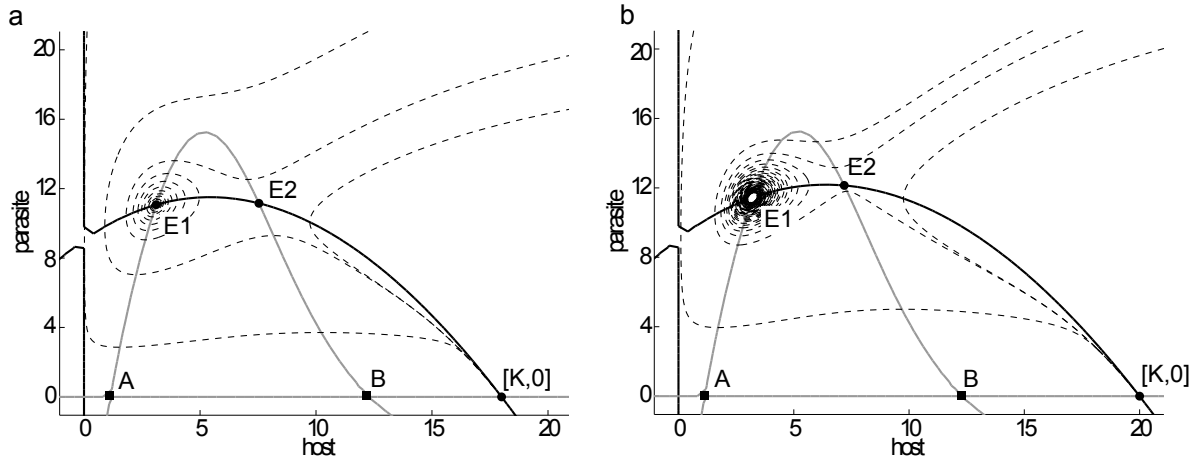

Figure 6: Phase plane of two stability cases for an equilibrium point E1. The host and hemiparasite isoclines refer to black and grey solid lines, respectively. Dashed lines denote oriented trajectories of the model (11). The equilibrium $[K, 0]$ is always stable, $E1$ is stable (a) or unstable with a stable limit cycle around it (b), and the equlibrium $E2$ is always unstable. The parameters were set as follows: $e = 1$, $a = 0.63$, $b = 6$, $d = 8$, $m = 0.1$, $m_1 = 0.01$, $c = 0.1$, $z = 4$, $g_\infty = 0.1$, and for $K = 18$ (a) and $K = 20.3$ (b).

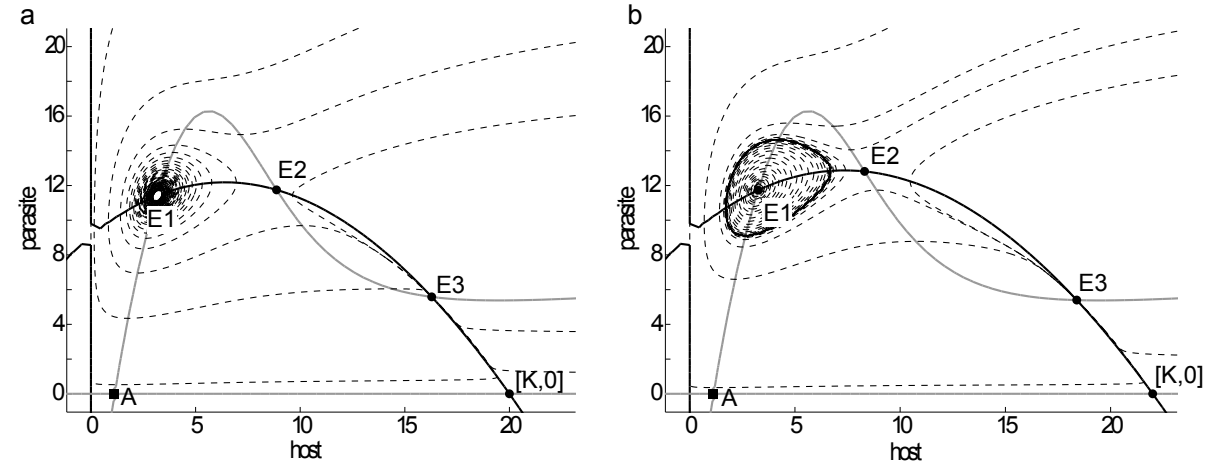

Figure 7: Phase plane of two stability cases for an equilibrium point E1. The host and hemiparasite isoclines refer to black and grey solid lines, respectively. Dashed lines denote oriented trajectories of the model (11). The equilibrium $[K, 0]$ and $E2$ is always unstable, $E1$ is stable (a) or unstable with a stable limit cycle around it (b), and $E3$ is always stable. The parameters were set as follows: $e = 1$, $a = 0.63$, $b = 6$, $d = 8$, $m = 0.1$, $m_1 = 0.01$, $c = 0.1$, $z = 4$, $g_\infty = 0.3$, and for $K = 20$ (a) and $K = 22$ (b).

4.4 *System dependence on parameters*

At first I investigated the dependence of the model (11) dynamics on the parameters involved in the original Rosenzweig-MacArthur predator-prey model (7). Then I examined the effect

of additional parameters introduced by Fibich et al. (2010). Finally, the parameters from the modified light availibility function $g(x)$ (10) and the host carrying capacity K were investigated.

An increase in parameter a, the maximum hemiparasite per capita "predation rate", causes a shift of the hemiparasite and host isoclines along the y axis up and down, respectively. Therefore, it extends the coexistence range where non-trivial equilibria exist. The same effect on the hemiparasite isocline has an increase in e, the efficiency of converting the host biomass into the hemiparasite biomass. Parameter b, the host biomass necessary to achieve one-half of the maximum rate a, has an opposite effect on the isoclines than parameter a. It shortens the coexistence range where non-trivial equilibria exist. Parameter m, the per capita mortality rate of predators in the absence of prey, determines the position of the hemiparasite isocline along the y axis, having an effect on the range of the coexistence equlibria.

Parameters added to the model by Fibich et al. (2010) also significantly affect its behaviour. An increase in parameter d, the host biomass necessary to achieve $g(x) = 1/2$, leads to the extension of the coexistence range by shifting the hemiparasite isocline up along both axes. Parameter c, the competitive ability of hemiparasites for light relative to their hosts, is negatively correlated with the carrying capacity of the host plant K in the presence of hemiparasites. Its increase causes a decrease of K. An increase in m_1 comprising intra-specific parasitism and competition for light moves the hemiparasite isocline maximum up along the hemiparasite axis causing the extend of the coexistence range.

Eventually, an increase in parameter g_∞ moves the maximum of the hemiparasite isocline along both axes up and thus it extends the coexistence range. It also changes the isocline shape for higher x when the second intersection with x axis, the point B, disappears and the isocline becomes positive. Parameter z influences the shape of the hemiparasite isocline as well. Its increase leads to a higher maximum of the hemiparasite isocline and faster decrease of the right (declining) side of the isocline. Therefore, it leads to the decrease of the coexistence range by moving the point B down along the x axis.

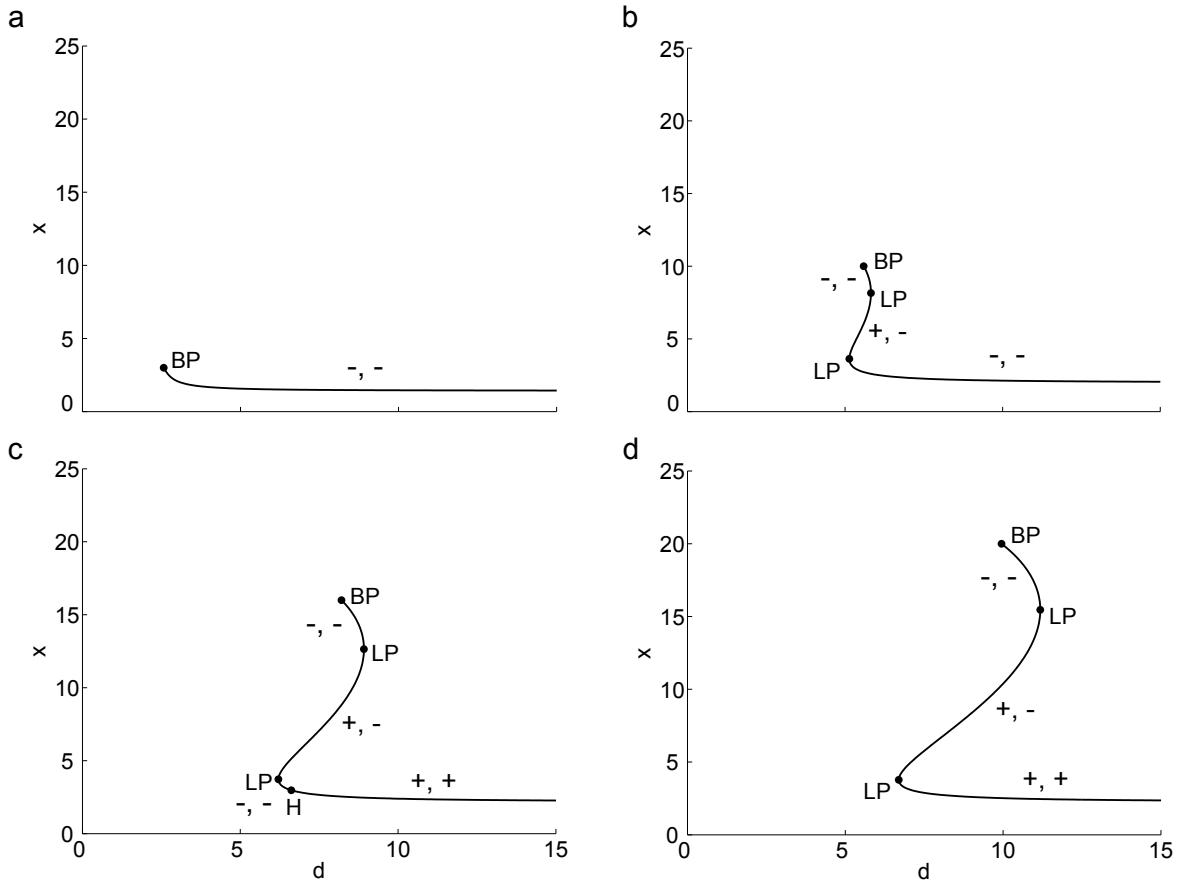

Figure 8: Bifurcation curves for parameter d, the host biomass necessary to achieve $1/2$ of $g(x)$, with respect to the host biomass x. Limit, Hopf and branching points are referred by LP, H and BP, respectively. Signs denote signs of the real parts of the eigenvalues of the corresponding Jacobian matrix. The parameters were set as follows: $e = 1$, $a = 0.63$, $b = 5$, $m = 0.1$, $m_1 = 0.01$, $c = 0.1$, $z = 2$, $g_\infty = 0$ and for $K = 3$ (a), $K = 10$ (b), $K = 16$ (c), $K = 20$ (d).

4.5 *Bifurcation analysis*

Bifurcation curves for parameter d with respect to the host biomass x show that the quantity and stability of equilibria is changing with increasing the host carrying capacity K (Fig. 8). While there is only one stable equilibrium under low K, one or two more equilibria exist under higher K (Fig. 8). To determine the areas of varying quantity and stability of equilibria more precisely, I displayed these bifurcation curves in a bifurcation diagram along the host carrying capacity K (Fig. 9a). Similar bifurcation diagrams were made for different values of parameters z and g_∞ (Fig. 9b-d).

When only g_∞ is increased, the shape of the branching point curve (BP curve) significantly changes and the limit point curve (LP curve) moves up along the x axis. This causes an

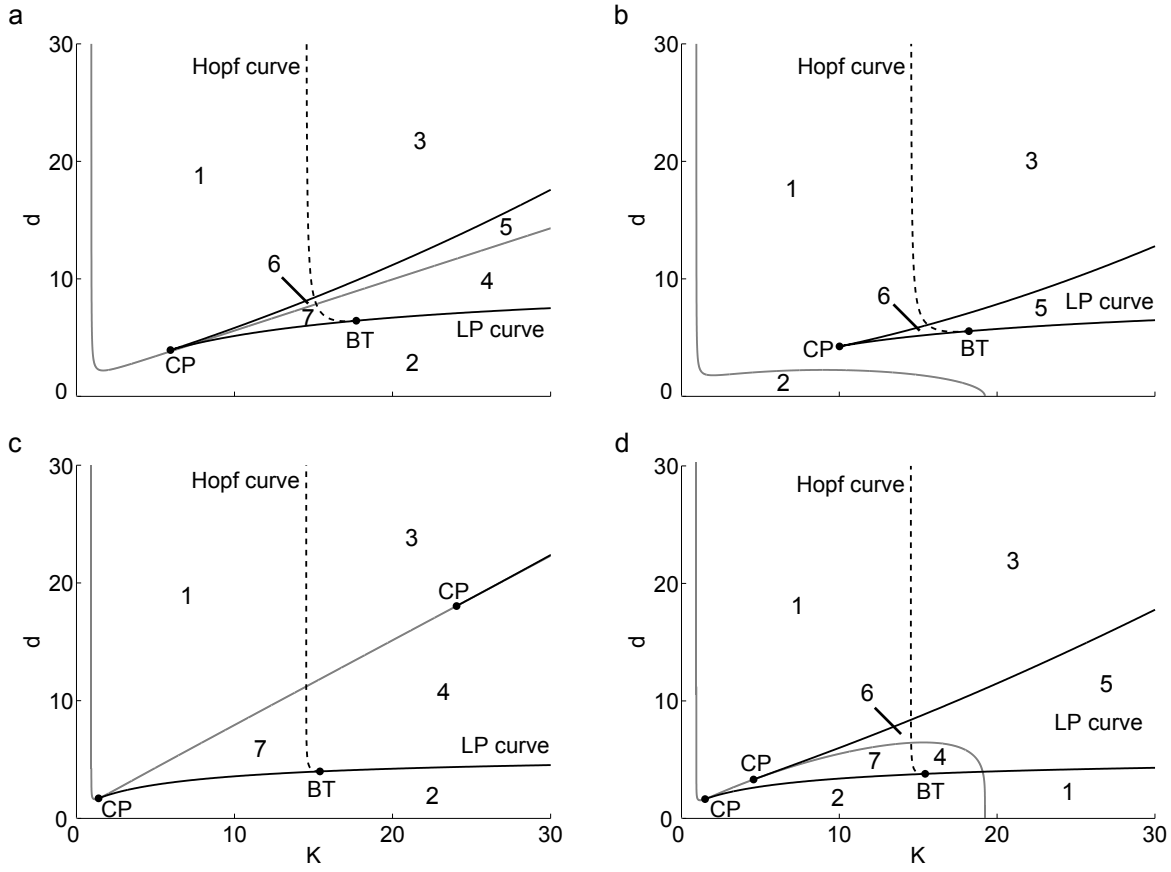

Figure 9: Bifurcation analysis of the coexistence equilibria of the model (11) for parameter d, the host biomass necessary to achieve $1/2$ of $g(x)$, along the host carrying capacity K. Black and grey solid lines refer to the limit point and branching point curves, respectively. Limit point curves delimit the areas where the equilibrium $E2$ exists. Branching point curves are a set of points at which the biomass of the parasite becomes zero. Dashed lines are the Hopf point curves. The Hopf point curves delimit the areas where the equilibrium $E1$ is unstable and surrounded by a stable limit cycle from the areas where $E1$ is stable. Cusp and Bogdanov-Takens bifurcation points further describing system stability are displayed as CP and BT, respectively. Numbers highlight the areas with various quantity and stability of equilibria. Area 1 denotes the area where the only coexistence equilibrium is stable equilibrium $E1$. In area 2, only stable trivial equilibrium $[K, 0]$ exists. In area 3, there is only an unstable coexistence equilibrium $E1$ which is surrounded by a stable limit cycle. Area 4 denotes the area where the trivial equilibrium $[K, 0]$ is stable, the equlibrium $E1$ is an unstable coexistence equilibrium, and $E2$ is an unstable saddle point. In area 5, $E1$ is an unstable coexistence equilibrium, $E2$ is an unstable saddle point, and $E3$ is stable or unstable. In area 6, $E1$ is a stable equilibrium and the stability of $E2$ and $E3$ is the same as in area 5. In area 7, stable equilibria $[K, 0]$ and $E1$, and an unstable saddle point $E2$ exist. The parameters were set as follows: $e = 1$, $a = 0.63$, $b = 5$, $m = 0.1$, $m_1 = 0.01$, $c = 0.1$, $z = 2$ (a, b) or $z = 5$ (c, d) and $g_\infty = 0$ (a, c) or $g_\infty = 0.2$ (b, d).

increase in area 1 where one stable equilibrium exists, and a decrease in the areas of multiple equilibria (Fig. 9a, b). Although some areas (3, 5, and 6) of coexistence equilibria increase

under higher g_∞, some (4 and 7) entirely disappear (Fig. 9a, b).

An increase of parameter z moves LP curve down along the x axis and therefore increases areas 4 and 7 inside the bifurcation fork where multiple equilibria exist (Fig. 9a, c). In these areas, $[K, 0]$ is a stable equilibrium, $E1$ is a stable or unstable equilibrium, and $E2$ is a saddle point. In addition, LP curve and BP curve almost merge under increased z leading to the disappearance of areas 5 and 6, the remaining areas of multiple equilibria (Fig. 9c).

The bifurcation diagram for which both parameters were increased combines the trends observed under the increase of only one parameter. The shape of BP curve significantly changes and the bifurcation fork moves down along the x axis slightly increasing the area of multiple equilibria (Fig. 9). All areas of multiple equilibria exist (Fig. 9). An increase of both g_∞ and z causes the decrease of the only trivial equilibrium area, area 2 (Fig. 9).

Finally, a homoclinic bifurcation curve further distinguishing the areas of multiple equilibria was detected during the bifurcation analysis (not shown). Once a stable limit cycle hits this curve (or more precisely the corresponding homoclinic loop), the limit cycle ceases to exist. However, since the issue of homoclinic bifurcation is above the level of knowledge of an undergraduate student, I will not examine this type of system behaviour here.

5 Discussion

The presented and analyzed model (11) is derived from the model of hemiparasite-host interaction by Fibich et al. (2010)(8), an extension of the well-known Rosenzweig-MacArthur predator-prey model (7) (Berryman, 1992; Kot, 2001; Pastor, 2008). Fibich et al. (2010) showed that the addition of the light availability function (9), a function introducing shading of the parasite by the host, to the model made the model more realistic. Here, I modified this function into a more general form (10) and similarly as Fibich et al. (2010) examined the hemiparasite-host coexistence along a productivity gradient of the environment. The productivity of the environment corresponded to the carrying capacity of the environment for the host species (K). The generalization involved the function exponent, parameter z, and the limit of the function when host biomass approach the infinity, parameter g_∞. Initial values of these parameters were set to $z = 2$ and $g_\infty = 0$, which resulted in the model of Fibich et al. (2010).

Isocline analysis provided various results depending on the value of parameter g_∞, which determined the shape of the hemiparasite isocline and existence (or not) of the second intersection point, the point B. If the point B exists ($g_\infty < \frac{m}{ea}$, 19), all coexistence equilibria lie at the intermediate K suggesting the coexistence of both species only under intermediate productivity of the environment. The species are not able to coexist under low and high environment productivities resulting in the extinction of the hemiparasite due to insufficient host biomass and strong light competition imposed by the host, respectively. This is consistent with the findings of Fibich et al. (2010). However, if the point B does not exist ($g_\infty > \frac{m}{ea}$, 18), the behaviour of the model especially for higher values of K is different. Whereas no coexistence equilibria were observed for high K and low g_∞, there is always a stable coexistence equilibrium for high K and sufficiently high g_∞. Fibich et al. (2010) observed similar behaviour regarding the coexistence of both species under high productivity after the exclusion of the hemiparasite shading by the host. However, this behaviour is not realistic when compared with field observations reporting the absence of many hemiparasitic species from highly productive sites (Hadač, 1969; Mudrák and Lepš, 2010; Hejcman et al., 2011). It is probably caused by underestimating light competition imposed by the host vegetation and affecting the hemiparasite biomass and its existence. Therefore, it rather corresponds to the behaviour of holoparasites, which do not depend on light for their growth. In addition, parameter z also influences the

shape of the hemiparasite isoclines and shortens the range (A, B) when B exists, but its effect on the model behaviour is not so profound as in the case of g_∞.

Bifurcation analysis showed that the number of coexistence equilibria increases with increasing the host carrying capacity K and their stability changes as well (Fig. 8). Both parameters markedly affect the areas of different quantity and stability of equilibria within the bifurcation diagrams (Fig. 9). Major effects induced by changing both parameters (g_∞ and z) or either of them are the modification of the areas of multiple equilibria and the decrease of the area where only the trivial equilibrium exists (area 2, Fig. 9).

If the second intersection point of the hemiparasite isocline with the x axis exists, the model results are in agreement with the results of two recent models examining the host-hemiparasite interaction. The non-spatial model of Cameron et al. (2009) revealed stable dynamics under low-nutrient levels, but unstable dynamics under high-nutrient levels suggesting the coexistence of hemiparasites and hosts only under low-nutrient levels. The extinction of the hemiparasite under the high productivity of the environment was also confirmed by Fibich et al. (2010). In contrast, if there is only one intersection point of the hemiparasite isocline with the x axis, the model results indicating stable dynamics under the high productivity of the environment are not in agreement with the results of both studies. Additionaly, another type of bifurcation was revealed in the presented and analyzed model under the initial parameter values set by Fibich et al. (2010): a homoclinic bifurcation. This is the bifurcation when a stable limit cycle surrounding an unstable equilibrium collides with a saddle point.

The Rosenzweig-MacArthur model including a carrying capacity of the prey (7) generally exhibits rather simple dynamics. However, certain extensions of the model can rapidly change its behaviour leading to more complex dynamics, when global bifurcations emerge (Zhu et al., 2002). A bifurcation describes a qualitative change of the model dynamics caused by a small change in the model parameter (Kuznetsov, 2010). A complex dynamical behaviour was also observed for the presented and analyzed model (11) comprising several forms of bifurcation – a fold, cusp, Hopf, Bogdanov–Takens, and homoclinic bifurcations. Similarly complex dynamics were recently found in other ecological models (e.g. Baer et al., 2006; Lade et al., 2013; Aguirre et al., 2014; Přibylová and Berec, 2014). Fold and cusp bifurcations were revealed in the model by Lade et al. (2013) regarding the human influence on regime-shifts

of the populations. Even richer bifurcation structure was identified in a two-stage population model (Baer et al., 2006), in a predator-prey model involving a strong Allee effect (Aguirre et al., 2014), and in a predator-interference model (Přibylová and Berec, 2014).

A mathematical model tries to describe a real system that we are focused on in its simplified form. This simplification is essential when we aim to understand and explain general patterns. Even the presented and analyzed model was designed assuming many simplifications. One of these simplifications concerns the characterization of host and hemiparasite populations exclusively by their biomasses. Therefore, the biomass increase cannot be further interpreted, e.g. as a new seedling emergence or the increase of the size of individual plant. Moreover, the extent of competition and parasitism depending purely on biomass is another simplification, which enables the model application only to short, herbaceous vegetation growing in the same vegetation layer. Furthermore, the model neglects any seasonality regarding the amount of biomass, rate of growth, competition, parasitism, and mortality. As these variables are species-specific, the incorporation of seasonality to the model will result in the loss of model generality.

Under higher values of g_∞, the presented and analyzed model (11) does not respond to field observations and provides unrealistic results. There are other ways of making the original model more realistic. As the light requirements of the hemiparasite differ according to its developmental stage (light competition is crutial especially in the seedling stage (Hejcman et al., 2011; Petrů and Lepš, 2000)), it would be appropriate to structure the hemiparasite population by age (seedlings vs. adult plants). In addition, water and mineral nutrients are usually considered as two different resources, which are taken up by plants. The separation of water and nutrient resource pool to two distinctive resources seems to be crucial according to the findings of Těšitel et al. (2014). They provided evidence about the interactive effect of mineral nutrients and water availability on the fundamental parameters of the host-hemiparasite association and highlighted the importance of experiments manipulating both of these resources. As hemiparasitic plants commonly grow in open habitats parasitizing many host species simultaneously and co-occuring with other non-host species, the addition of more host or non-host autotrophic plant species to the model is another way of improving the model.

6 Conclusions

The presented and analyzed model examining the hemiparasite-host coexistence along a productivity gradient showed a complex dynamical behaviour comprising several forms of bifurcation. The number of coexistence equilibria increased with increasing the host carrying capacity K and their stability changed as well. Both generalized parameters of the light availability function (the parameters g_∞ and z) markedly affected the areas of different quantity and stability of equilibria. Especially, parameter g_∞ was shown to significantly affect the model behaviour. Under lower values of g_∞ ($g_\infty < \frac{m}{ea}$), the behaviour of the model was consistent with the original model and with field observations reporting the absence of many hemiparasitic species from highly productive sites. All coexistence equilibria lied at the intermediate values of K suggesting the coexistence of both species only under intermediate productivity of the environment. However, the behaviour of the model was not in agreement with the original model and field observations under higher values of g_∞ ($g_\infty > \frac{m}{ea}$), when the model reached stable dynamics even under the high productivity of the environment. Such an unrealistic result was probably caused by an underestimation of light competition imposed by the host vegetation and affecting the hemiparasite biomass and its existence.

References

Aguirre, P., J. D. Flores, and E. González-Olivares. 2014. Bifurcations and global dynamics in a predator–prey model with a strong Allee effect on the prey, and a ratio-dependent functional response. Nonlinear Analysis: Real World Applications 16:235–249.

Ameloot, E., K. Verheyen, and M. Hermy. 2005. Meta-analysis of standing crop reduction by *Rhinanthus* spp. and its effect on vegetation structure. Folia Geobotanica 40:289–310.

Atsatt, P., and D. Strong. 1970. The population biology of annual grassland hemiparasites. I. The host environment. Evolution 24:278–291.

Baer, S. M., B. W. Kooi, Y. A. Kuznetsov, and H. R. Thieme. 2006. Multiparametric bifurcation analysis of a basic two-stage population model. SIAM Journal on Applied Mathematics 66:1339–1365.

Bardgett, R. D., R. S. Smith, R. S. Shiel, S. Peacock, J. M. Simkin, H. Quirk, and P. J. Hobbs. 2006. Parasitic plants indirectly regulate below-ground properties in grassland ecosystems. Nature 439:969–972.

Berryman, A. 1992. The origins and evolution of predator-prey theory. Ecology 73:1530–1535.

Cameron, D. D., A. M. Coats, and W. E. Seel. 2006. Differential resistance among host and non-host species underlies the variable success of the hemi-parasitic plant *Rhinanthus minor*. Annals of Botany 98:1289–1299.

Cameron, D. D., J.-K. Hwangbo, A. M. Keith, D. Kraushaar, J. Rowntree, and W. E. Seel. 2005. Interactions between the hemiparasitic angiosperm *Rhinanthus minor* and its hosts: from the cell to the ecosystem. Folia Geobotanica 40:217–229.

Cameron, D. D., and W. E. Seel. 2007. Functional anatomy of haustoria formed by *Rhinanthus minor*: linking evidence from histology and isotope tracing. New Phytologist 174:412–419.

Cameron, D. D., A. White, and J. Antonovics. 2009. Parasite-grass-forb interactions and rock-paper-scissor dynamics: predicting the effects of the parasitic plant *Rhinanthus minor* on host plant communities. Journal of Ecology 97:1311–1319.

Davies, D., J. Graves, C. Elias, and P. Williams. 1997. The impact of *Rhinanthus* spp. on sward productivity and composition: implications for the restoration of species-rich grasslands. Biological Conservation 82:87–93.

De Hullu, E. 1984. The distribution of *Rhinanthus angustifolius* in relation to host species. Pages 43–53 in C. Parker, L. Musselman, R. Polhill, and A. Wilson, eds. Proceedings of the 3rd International Symposium on Parasitic weeds. IACARDA, Aleppo, Syria.

Demey, A., T. Rütting, D. Huygens, J. Staelens, M. Hermy, K. Verheyen, and P. Boeckx. 2014. Hemiparasitic litter additions alter gross nitrogen turnover in temperate semi-natural grassland soils. Soil Biology and Biochemistry 68:419–428.

Dhooge, A., W. Govaerts, and Y. A. Kuznetsov. 2003. MATCONT: A Matlab package for numerical bifurcation analysis of ODEs. ACM Trans Math Software (TOMS) 29:141–164.

Fibich, P., J. Lepš, and L. Berec. 2010. Modelling the population dynamics of root hemiparasitic plants along a productivity gradient. Folia Geobotanica 45:425–442.

Fürst, F. 1931. Der Klappertopf als Acker- und Wiesenunkraut. Archiv für Pflanzenbau 6:28–141.

Gibson, C., and A. Watkinson. 1991. Host selectivity and the mediation of competition by the root hemiparasite *Rhinanthus minor*. Oecologia 86:81–87.

Grime, J. 1979. Plant strategies and vegetation processes. Wiley, New York.

Hadač, E. 1969. Die Pflanzengesellshaften des Tales “Dolina Siedmich prameňov" in der Belaer Tatra. Vydavate‘lstvo Slovenskej Akadémie Vied, Bratislava.

Heide-Jørgensen, H. 2013. Introduction: The parasitic syndrome in higher plants. Chap. 1, pages 1–14 in D. Joel, J. Gressel, and L. Musselman, eds. Parasitic Orobanchaceae: Parasitic mechanisms and control strategies. Springer-Verlag, Berlin, Heidelberg.

Hejcman, M., J. Schellberg, and V. Pavlů. 2011. Competitive ability of *Rhinanthus minor* L. in relation to productivity in the Rengen Grassland Experiment. Plant, Soil and Environment 57:45–51.

Irving, L. J., and D. D. Cameron. 2009. You are what you eat: interactions between root parasitic plants and their hosts. Advances in Botanical Research 50:87–138.

Joshi, J., D. Matthies, and B. Schmid. 2000. Root hemiparasites and plant diversity in experimental grassland communities. Journal of Ecology 88:634–644.

Keddy, P., L. Twolan-Strutt, and B. Shipley. 1997. Experimental evidence that interspecific competitive asymmetry increases with soil productivity. Oikos 80:253–256.

Kot, M. 2001. Elements of mathematical ecology. Cambridge University Press, Cambridge.

Kuznetsov, Y. A. 2010. Elements of applied bifurcation theory. 2nd ed. Springer, New York.

Lade, S. J., A. Tavoni, S. A. Levin, and M. Schlüter. 2013. Regime shifts in a social-ecological system. Theoretical Ecology 6:359–372.

Matthies, D. 1995. Parasitic and competitive interactions between the hemiparasites *Rhinanthus serotinus* and *Odontites rubra* and their host *Medicago sativa*. The Journal of Ecology 83:245–251.

Mudrák, O., and J. Lepš. 2010. Interactions of the hemiparasitic species *Rhinanthus minor* with its host plant community at two nutrient levels. Folia Geobotanica 45:407–424.

Pastor, J. 2008. Mathematical ecology of population and ecosystems. Wiley, Chichester.

Perko, L. 2001. Diferential equations and dynamical systems. 3rd ed. Springer, New York.

Petrů, M., and J. Lepš. 2000. Regeneration dynamics in populations of two hemiparasitic Pedicularis species in wet grasslands. Pages 329–333 in P. White, L. Mucina, and J. Lepš, eds. Vegetation science in retrospect and prospective. Opulus Press, Uppsala.

Polking, J., and D. Arnold. 1999. Ordinary differential equations using MATLAB. Prentice Hall, Upper Saddle River, NJ.

Prati, D., D. Matthies, and B. Schmid. 1997. Reciprocal parasitation in *Rhinanthus serotinus*: a model system of physiological interaction in clonal plants. Oikos 78:221–229.

Press, M. 1989. Autotrophy and heterotrophy in root herniparasites. Trends in Ecology & Evolution 4:258–263.

Press, M. C. 1998. Dracula or Robin Hood? A functional role for root hemiparasites in nutrient poor ecosystems. Oikos 82:609–611.

Press, M. C., and G. K. Phoenix. 2005. Impacts of parasitic plants on natural communities. New Phytologist 166:737–751.

Pywell, R. F., J. M. Bullock, K. J. Walker, S. J. Coulson, S. J. Gregory, and M. J. Stevenson. 2004. Facilitating grassland diversification using the hemiparasitic plant *Rhinanthus minor*. Journal of Applied Ecology 41:880–887.

Přibylová, L., and L. Berec. 2014. Predator interference and stability of predator-prey dynamics. Journal of Mathematical Biology .

Quested, H. M., T. V. Callaghan, J. H. C. Cornelissen, and M. C. Press. 2005. The impact of hemiparasitic plant litter on decomposition: direct, seasonal and litter mixing effects. Journal of Ecology 93:87–98.

Rosenzweig, M., and R. MacArthur. 1963. Graphical representation and stability conditions of predator-prey interactions. American Naturalist 97:209–223.

Rümer, S., D. D. Cameron, R. Wacker, W. Hartung, and F. Jiang. 2007. An anatomical study of the haustoria of *Rhinanthus minor* attached to roots of different hosts. Flora 202:194–200.

Smith, D. 2000. The population dynamics and community ecology of root hemiparasitic plants. American Naturalist 155:13–23.

Thorogood, C. J., and S. J. Hiscock. 2010. Compatibility interactions at the cellular level provide the basis for host specificity in the parasitic plant *Orobanche*. New Phytologist 186:571–575.

Těšitel, J., L. Plavcová, and D. D. Cameron. 2010. Heterotrophic carbon gain by the root hemiparasites, *Rhinanthus minor* and *Euphrasia rostkoviana* (Orobanchaceae). Planta 231:1137–1144.

Těšitel, J., T. Těšitelová, J. P. Fisher, J. Lepš, and D. D. Cameron. 2014. Integrating ecology and physiology of root-hemiparasitic interaction: interactive effects of abiotic resources shape the interplay between parasitism and autotrophy. New Phytologist 205:350–360.

Van Hulst, R., B. Shipley, and A. Theriault. 1987. Why is *Rhinanthus minor* (Scrophulariaceae) such a good invader? Canadian Journal of Botany 65:2373–2379.

Westwood, J. H. 2013. The physiology of the established parasite–host association. Pages 87–114 in D. Joel, J. Gressel, and L. J. Musselman, eds. Parasitic Orobanchaceae: Parasitic mechanisms and control strategies. Springer-Verlag.

Wilson, S. D., and D. Tilman. 1991. Component of plant competition along an experimental gradient of nitrogen availability. Ecology 72:1050–1065.

Yeo, P. 1964. The growth of *Euphrasia* in cultivation. Watsonia 6:1–24.

Zhu, H., S. Campbell, and G. Wolkowicz. 2002. Bifurcation analysis of a predator-prey system with nonmonotonic functional response. SIAM Journal on Applied Mathematics 63:636–682.